中國機械工程學刊第三十六卷第一期第41~48頁(民國一百零四年)
Journal of the Chinese Society of Mechanical Engineers, Vol.36, No.1, pp 41~48 (2015)

An Investigation into Suitable Friction Factor and Optimized Forming Process of 6061 Aluminum Alloy Bicycle Stem

Dyi-Cheng Chen*, Jheng-Guang Lin**, Yu-Ting Chu** and Jiun-Ru Shiu**

Keywords: Aluminum alloy bicycle stem, Forming process, Friction factor

ABSTRACT

The friction factor is a crucial parameter in metal forming, and it affects the billet forming process. This paper discusses the AL6061 aluminum friction factor based on the results of a ring crush test. Experimental and simulation compression ratios were combined in this study to draw graphs by using these friction values. Finally, DEFORM^{TM}3D software was used to analyze the impact of the various experimental parameters that were involved in forming a bicycle stem, to explore the effective stress, effective strain, axial force, velocity field, and observed micro-grain products, and to simulate and conduct size comparison experiments. The results of the analysis can be used to stabilize the finite element software that is used to form bicycle stems.

INTRODUCTION

Global awareness of environmental issues and green energy has gradually increased, prompting people to use bicycles as a means of transportation. Riding a bicycle is environmentally friendly, healthy, and alleviates environmental pollution. Most high-priced bicycles are composed of a light metal. Aluminum alloys are light, highly dense, and easily recycled. Therefore, aluminum is often used in the bicycle industry. This study developed a lightweight bicycle stem, because the stem of a bicycle affects the design and manufacture of safe and comfortable bicycles. The minimization of excess material and increased structural strength of a one-piece ergonomic product line were also investigated.

According to the weight reduction evaluations that were conducted, high-strength aluminum alloys, such as A7075, could be used to replace high-strength steel (Huang et al. 2010). Béland (2009) used the finite element method to optimize die and mandrel geometry in tube drawings of tubes that exhibited a constant thickness. Guillot et al. (2010) tested a range of aluminum alloys and various mandrel geometries. However, these experiments were expensive and time consuming. Prasad and Rao modeled the isothermal forging of a rib–web shaped component exhibited in electrolytic copper. This was achieved using the material models in a finite element simulation. They then used laboratory forging trials to validate their results (Prasad and Rao, 2011). Chen et al. (2013) examined the innovative forging process by using simulation analyses of varying ram press velocities, die temperatures, and die friction factors to evaluate weight quantification methods for forging bicycle pedals. Chen et al. (2013) analyzed an innovative forging mold design for various bicycle stems. They combined the Taguchi method with the artificial neural network algorithm to identify the best design parameters.

The friction factor is a crucial parameter regarding metal forming and it also affects the billet forming process. This study used the friction factor to explore the bicycle stem forming process to identify the most favorable friction factors that occur during formation. Nakamura and Ishibashi (2010) proposed using double-layer dry-in-place type lubricants. These solid lubricant films were composed of an undercoat (exhibiting a high level of adherence to materials) and an overcoat (exhibiting favorably reduced friction). Sliding virgin lubricant layers were achieved only when the entire sliding surface of the tool and specimen did not make simultaneous contact. This eliminated ring-shaped geometry. The active

Paper Received August, 2014. Revised October, 2014. Accepted December,2014. Author for Correspondence: Dyi-Cheng Chen

**Professor, Department of Industrial Education and Technology, National Changhua University of Education, Changhua 500, Taiwan.*

*** Graduate Student, Department of Industrial Education and Technology, National Changhua University of Education, Changhua 500,Taiwan.*

tool surface must be plain analysis to avoid an additional plastic specimen deformation leading to inaccurate measurements being recorded during sliding (Buchner et al, 2008). The friction factor that was created using the rigid-plastic finite element DEFORM-3D software is shown in Table 3 (DEFORM^{TM} 3D, 2006).

This paper focuses on experimental parameters including effective stress, effective strain, and axial force. The results of the analysis can be used to stabilize the finite element software that is used to form bicycle stems.

DIE DESIGN

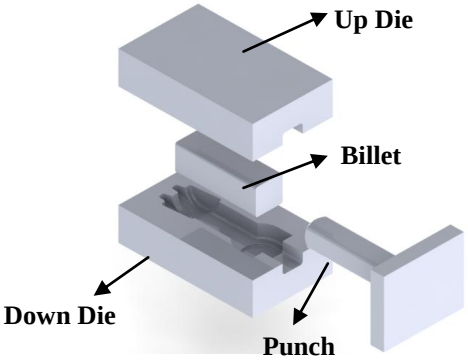

Fig. 1. Die combination chart

In this study, 3D graphics software, Soildwork, was used to design and model the bike riser mold components that are shown in Fig. 1. The design was then implemented using a CNC milling machine for production processing. The shape of the molds that were produced are displayed in Fig. 2.

Fig. 2. Schematic of bicycle stem mold

EXPERIMENTAL METHODS

This study used the ring crush friction test to obtain the friction factor between the mold and the billet. Because the friction factor affects the metal molding process, when the billet in the mold produces mobility, it affects the size of the friction billet. Therefore, obtaining the correct friction factor is critical. An A6061 aluminum alloy test piece was used in this study. The ratio of the outer diameter to the inner diameter to the height of the test piece was 6:3:2, or 36 mm × 18 mm × 12 mm. The process machine tools traditionally used in lathe turning precision may have produced small errors. The applied experimental conditions are listed in Table 1. The A6061 mechanical properties used from the software.

Table 1. Experimental conditions of ring test

Specimen No.	1	2	3
The inner diameter of the specimen	18.03	18.00	17.98
Height dimensions of the specimen	12.05	11.97	12.03
High compression ratio	22.8%	31.1%	41.8%
Die material	SKD61		
Blank material	A6061		
Die, billet temperature	20°C		
Punch speed	10mm/min		
Lubricant	Graphite		

Before the experiment, finite element analysis software, DEFORM-3D, was used to create a friction graph. The analysis of the simulation involved establishing the necessary mold material, blank material, temperature, and punch speed, as shown in Table 1. Only the friction factor was changed (m = 0.05) to simulate the effects of diameter change on variations in volume and height. The inner diameter of the compression ratio and the high-compression ratio formula were simultaneously calculated using (1) and (2), respectively, producing the friction curve shown in Fig. 3.

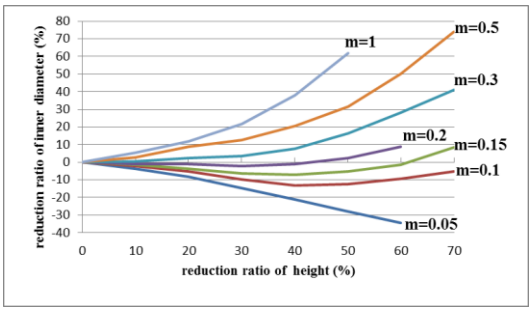

Fig. 3. Friction factor graph using DEFORM 3D software

The reduction ratio of the inner diameter is calculated as follows:

$$\frac{D_I - D}{D_I} \times 100\% \qquad (1)$$

where D_I is the precompressed inner diameter and D is the inner diameter after compression.

The reduction ratio of height is calculated as follows:

$$\frac{H_O - H}{H_O} \times 100\% \qquad (2)$$

where H_O is the precompression height and H is the height after compression.

The maximum load of an 80-ton universal testing machine was used to rotate a test piece of A6061 aluminum alloy, which was sprayed using graphite lubricant at a compression speed of 10 mm/min, as shown in Fig. 4. Fig. 5 displays the compressed specimens that were removed. The specimen measurement results are listed in Table 2, indicating the optimal results, inner diameter compression ratio, and high-compression ratios. The friction simulation graph reflected a friction factor of 0.2, as illustrated in Fig. 6.

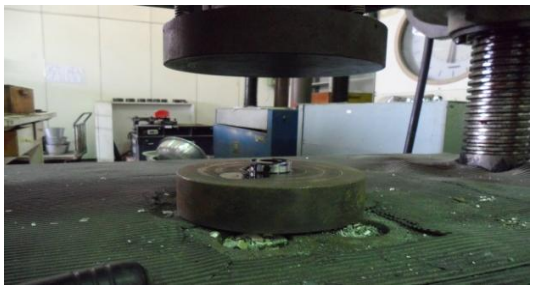

Fig. 4. Experimental procedure of A6061

Fig. 5. Ring test of A6061

SIMULATION RESULTS AND ANALYSIS

Fig. 7 depicts the relationship between true stress and true strain in A6061 aluminum alloy. Table 3 lists the simulation parameters that were set to test the effects of effective stress, effective strain, and Z load.

Table 2. Measurement results of ring test

Specimen No.	Original diameter	Original Height	The compressed
	size (mm)	Dimensions (mm)	diameter size (mm)
1	18.03	12.05	18.07
2	18.00	11.97	18.08
3	17.98	12.03	17.85

Specimen No.	The compressed height dimension (mm)	The inner diameter of the compression ratio (%)	The high compression ratio (%)
1	9.3	-0.22	22.8
2	8.25	-0.44	31.1
3	7	0.72	41.8

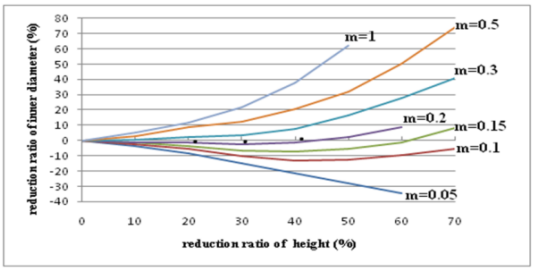

Fig. 6. Friction factor curve calibration graph using A6061 experiment

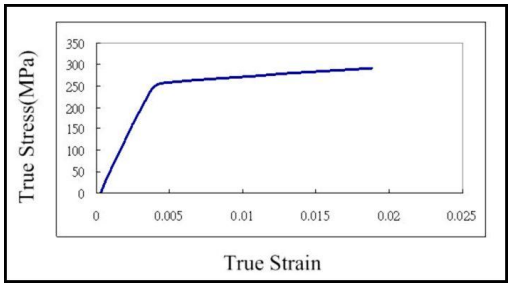

Fig. 7. A6061 relationship of true stress and true strain

Table 3. Parameters setting of simulation analysis

Experiment	Product angle θ	Friction factor	Die temperature (°C)	Forging speed (mm/sec)
1	2	0.2	300	10
2	4	0.2	300	10
3	6	0.2	300	10
4	6	0.3	300	10
5	6	0.5	300	10
6	6	0.5	400	10
7	6	0.5	500	10
8	6	0.5	500	20
9	6	0.5	500	30

Fig. 8 shows the Z Load regarding the various process conditions of the bicycle stem, indicating that Experiment 3 produced the largest Z load. Higher mold temperatures were generated in Simulations 7, 8, and 9, which used smaller loads. Thus, the mold temperature affected the forging process.

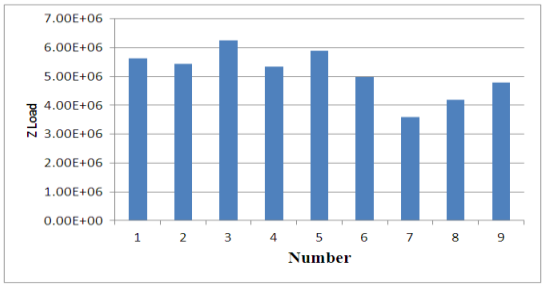

Fig. 8. Z Load of different process conditions of the bicycle stem

Fig. 9 illustrates the effective stress regarding different process conditions of the bicycle stem. The effective stress, product angle, friction factor, and forging speed did not affect the stress. Simulations 5, 6, and 7 revealed that temperature affected the effective stress. Fig. 10 shows that the punch pressure head and the front section of the bicycle stem produced an effective strain.

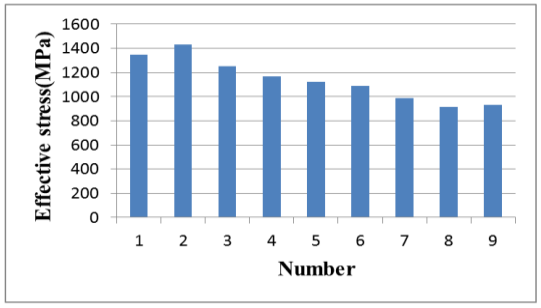

Fig. 9. Effective stress of different process conditions of the bicycle stem

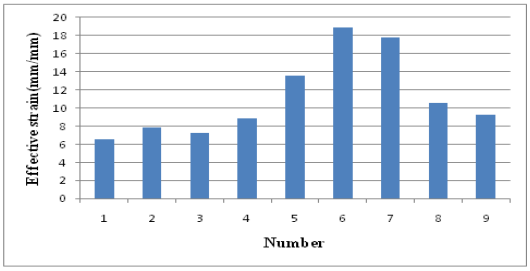

Fig. 10. Effective strain of different process conditions of the bicycle stem

Figs. 11 and 12 illustrate the effective stress and effective stain distributions exhibited during bicycle stem forming. The maximum effective stress reached to 914 MPa, and effective strain reached to 4.59 both occurred in front stem part. The die temperature parameters were set as listed in Table 4.

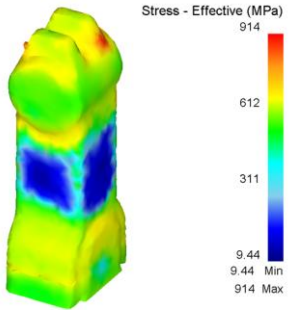

Fig. 11. Effective stress distributions of bicycle stem forming

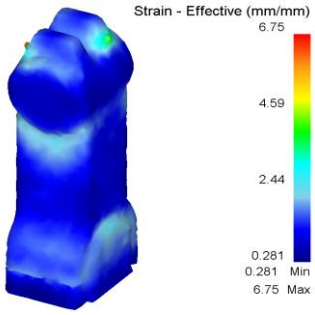

Fig. 12. Effective strain distributions of bicycle stem forming

Table 4. Die temperature parameter setting

Billet size (mm)	AL 6061, 40×40×115
Number of grids	50000
Die temperature (^{o}C)	500
Stem angle (^{o})	4
Punch speed (mm/sec)	10
Friction Factor	0.2

This study analyzed the bike vertical wall, as shown in Fig. 13. The dimensions were set as listed in Table 5. The fixed parameters were as follows: mold temperature = 500 ℃; punch head speed = 10 mm/sec; friction factor = 0.2; and t was set at the varying sizes of 1 mm, 2 mm, 3 mm, and 4 mm. As shown in Fig. 14, at t = 3 mm or 4 mm, the bicycle stem handlebar clamp terminals were completely filled. When t = 1 mm or 2 mm the process exhibited too little billet reflux, which caused the handlebar clamp end standpipe to fill incompletely. Therefore, including the choice of wall thickness t = 4 mm in the design parameters enhanced the strength of the standpipe.

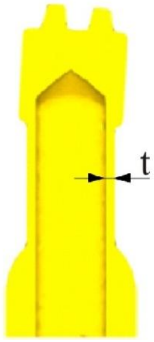

Fig. 13. Bicycle stem wall thickness t

Table 5. t-sized parameters set

Billet size (mm)	AL 6061, 40×40×115			
Number of grids	50000			
Die temperature (°C)	500			
Stem angle (°)	4			
Punch speed (mm/sec)	10			
Friction Factor	0.2			
t Size (mm)	1	2	3	4

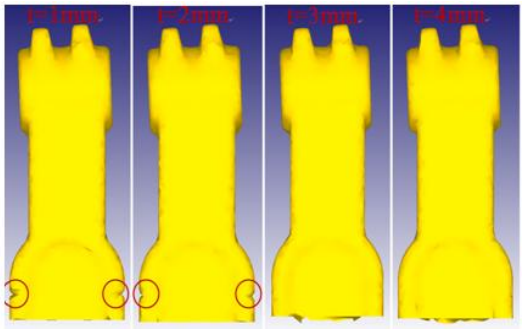

Fig. 14. A wall thickness of the finished reflux

The billet length, L, was set at the sizes listed in Table 6. The fixed parameters were as follows: mold temperature = 500 ℃; punch speed = 10 mm/sec; friction factor = 0.2; and the billet length (L) was set at the varying sizes of 100 mm, 115 mm, and 125 mm. As shown in Fig. 15, the length of the 100 mm billet that estimated not enough materials, leading the stem forming to be incomplete. Using the 125 mm billet resulted in a mold flash problem; setting the billet length at L = 115 mm regarding the bike stem forging simulation yielded favorable results.

Table 6. L size parameters setting

Billet size (mm)	AL 6061, 40×40×115		
Number of grids	50000		
Die temperature (°C)	500		
Stem angle (°)	4		
Punch speed (mm/sec)	10		
Friction Factor	0.2		
t Size (mm)	4		
L Size (mm)	100	115	125

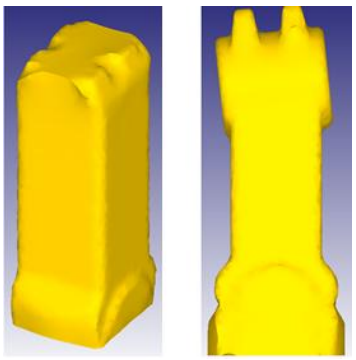

Fig. 15. Illustration of L size simulation

Finally, to optimize the parameters listed in Table 7, optimal parameters including stem angle 4°, punch speed 10 mm/sec, t size 4 mm, L size 115 mm; a mold-making and velocity field simulation was conducted (Figs. 16 (a) and 16 (b)) to analyze the billet velocity field expansion at the middle of the front and rear of bicycle stem. Fig. 16 (c) shows that the billet was formed at a slow speed to fill the mold gradually.

Table 7. Optimal parameter set

Billet size(mm)	AL 6061, 40×40×115
Number of grids	50000
Die temperature (℃)	500
Stem angle (°)	4
Punch speed (mm/sec)	10
Friction factor	0.2
t size (mm)	4
L size (mm)	115

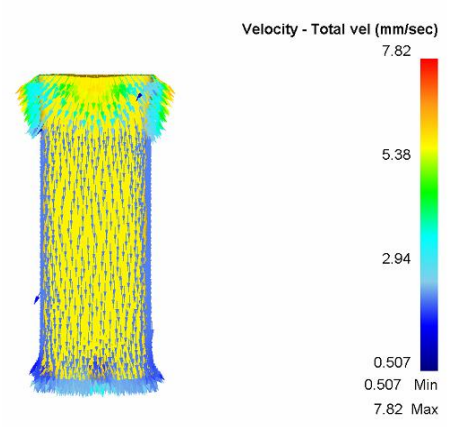

(a) before forming

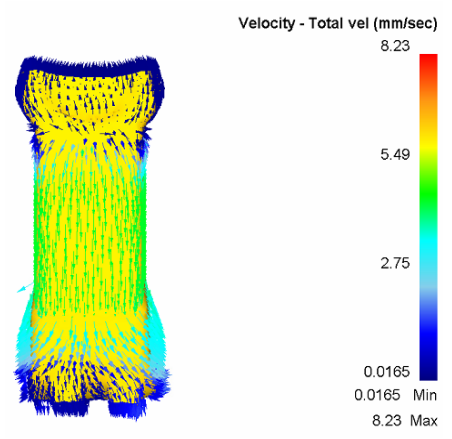

(b) during forming

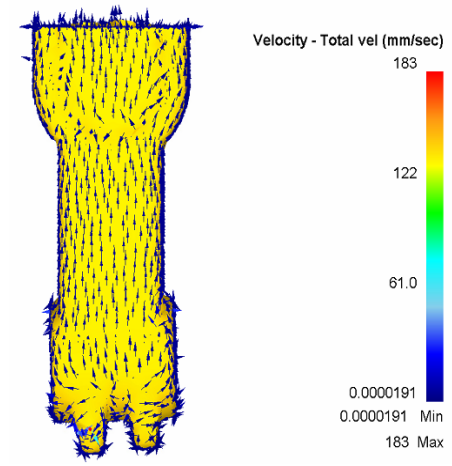

(c) after forming

Fig. 16. Forming velocity field

EXPERIMENTAL RESULTS

Forging experiment

The A6061 aluminum alloy was placed inside an upper and lower billet mold, the mold removal agent was sprayed onto the mold, and the mold was then placed in a mold punch which was then placed in a high-temperature furnace (Fig. 17) and heated to 500 ℃. Afterward, the forged aluminum was removed from the furnace and placed in a universal tensile test machine, as shown in Fig. 18.

The mold was pressed to seal it completely and was cooled to below 100 ℃; the form removal operation was then performed (Fig. 19). As illustrated in Fig. 20, when the process was complete, the material was removed, revealing that it thoroughly filled the mold. After the finished product was removed, a rasp burr was used to finalize the bike stem forging experiments.

Fig. 17. High temperature furnace

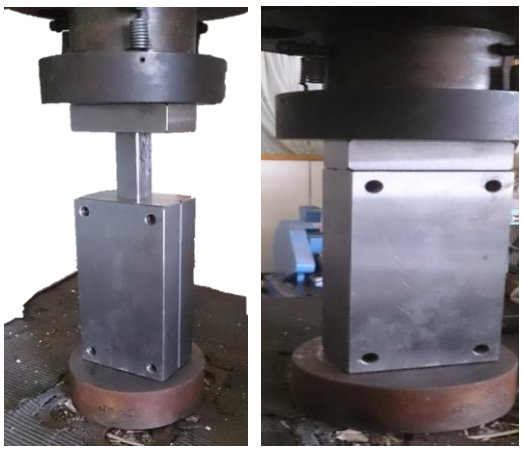

Fig. 18. Forging processing of bicycle stem

Fig. 19. Schematic of experimental processing

(a) analysis design (b) experiment product

Fig. 20. simulation and experimental design the finished product

Metallurgical results

The test pieces were finished parquet nodes that were buried and polished, as shown in Fig. 21.

Figs. 22 and 23 illustrate the results of the bicycle stem microstructure analysis that was conducted. This analysis revealed that the most delicate point was observed at P2, and the coarsest grains were observed at P3. The experiments enabled determining the forging of point P3 in the billet reflux area. The forging force at P3 was relatively small, resulting in unevenly coarse grains, whereas P2 exhibited enhanced wear and strength because it exhibited fine uniform grains.

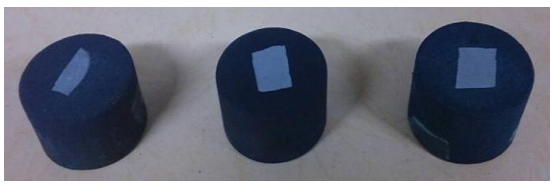

Fig. 21. Inserts buried node specimens

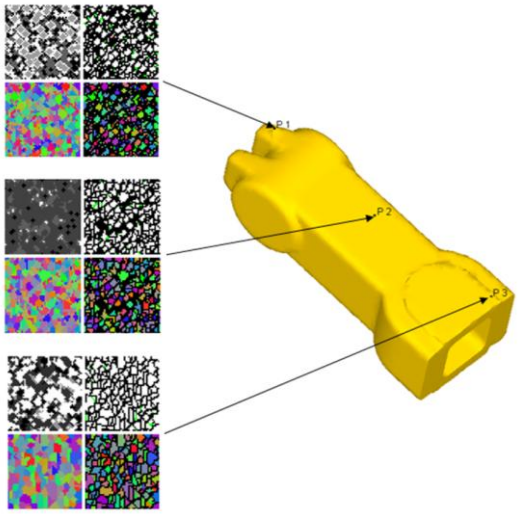

Fig. 22. Bicycle stem microstructure analysis chart

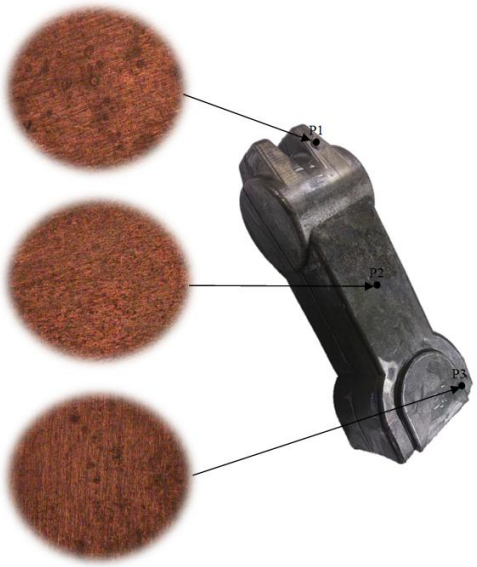

Fig. 23. Nodes observe the microstructure

To verify the feasibility of the finite element simulation and differences between the processes, the size of the finished product and the design approach were compared to the design dimensions shown in Fig. 24. Table 8 lists the size comparisons of the simulation and experiment.

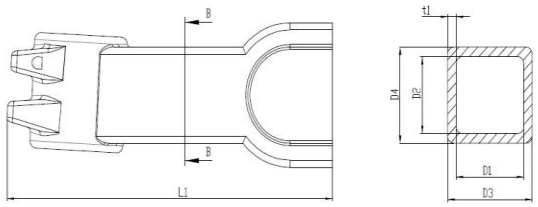

Fig. 24. Bicycle stem size design

Table 8 Dimension comparison of simulation and experiment

	Simulation size (mm)	Experiment size (mm)	Error(%)
L1	120.55	122.68	-1.736
t1	4.08	4.15	1.49
D1	40.20	40.15	0.12
D2	40.15	40.18	-0.075
D3	36.12	36.00	0.33
D4	36.07	36.03	-0.638

CONCLUSIONS

This study used finite element software to simulate the plastic deformation behavior of an aluminum alloy (AL6061) during the production of a bicycle stem. The results show that the optimal parameter settings for the forging process are: (a) a friction factor of 0.2 based on the ring compression test; (b) the punch pressure head and front portion of the bicycle stem exhibit the most effective stress; (c) the highest effective strain occurs during drilling and while forming the bicycle stem; (d) optimal parameters including stem angle 4^{o}, punch speed 10 mm/sec, t size 4 mm, L size 115 mm; and (e) the experimental results of the comparative analysis regarding the forging of a bicycle stem show that the simulation parameters predict the shape of the mold/die accurately.

ACKNOWLEDGMENT

The authors gratefully acknowledge the financial support of the National Science Council of the Republic of China under Grant No. NSC 101-2221-E-018-001.

REFERENCES

Beland, J.F., M.Sc. thesis, Laval University, Quebec, Canada (in French) (2009).

Buchner, B., Maderthoner, G. and Buchmayr, B., "Characterisation of Different Lubricants Concerning the Friction Coefficient in Forging of AA2618," *Journal of Materials Processing Technology*, Vol. 198, pp. 41-47 (2008).

Chen, D.C., Shiu, J.R. and Lin, J.G., "Optimization Analysis of A7075 Bicycle Stem Forging Process," *Key Engineering Materials*, Vol. 554-557, pp. 227-233 (2013).

Chen, D.C., Shiu, J.R., Nian, F.L. and Chen, M.R., "Analysis of Forging Forming of 6061 Aluminum Alloy Bicycle Pedal," *Applied Mechanics and Materials*, Vol. 271-272, pp. 31-35 (2013).

DEFORM^{TM} 3D, criterion DEFORM^{TM} 3D Version 6.1(sp1) Post-Processor Discrete Lattice Microstructure Modeling Lab, Scientific Forming Technologies Corporation, Columbus Normalized C (2006).

Guillot, M., Girard, S., D' Amours, G., Rahem, A. and Fafard, M., SAE 2010 World Congress, Detroit, USA (2010).

Huang, H., Li, D.Y. and Peng, Y.H., "Experimental Study on the Forming Limit Diagrams (FLD) of 7075-T6 Aluminum Alloy Sheet at Warm State," *Journal of Plasticity Engineering*, Vol. 17, No. 1, pp.93-97 (2010).

Nakamura, T. and Ishibashi, I., "Evaluation of Environmentally Friendly Lubricants for Cold Forging," Proceedings of the 11th Asian Symposium on Precision Forging, Kyoto, Japan, pp. 90 – 95 (2010).

Prasad, Y.V.R.K. and Rao, K.P., "Materials Modeling and Finite Element Simulation of Isothermal Forging of Electrolytic Copper," *Materials and Design*, Vol. 32, pp. 1851–1858 (2011).

6061 鋁合金自行車豎管適當摩擦因子與最佳成形加工

陳狄成、林政光、朱祐霆、許珺茹
國立彰化師範大學工業教育與技術學系

摘要

金屬成型加工中摩擦因子是一個重要的參數，同時影響胚料在模具中成形的過程，本文透過環壓試驗探討AL6061鋁合金摩擦因子，結合實驗與模擬的壓縮率來繪製曲線圖並得知摩擦數值，最後以DEFORM^{TM}3D軟體分析各實驗參數對自行車豎管鍛壓成形之影響，並探討豎管成型之等效應力、等效應變、軸向力、速度場及成形尺寸之比較，期望分析結果能穩定有限元素軟體對自行車豎管成形之可行性。